Submitted to the XXXth International Conference on High Energy Physics ICHEP2000,
Osaka, Japan, July 2000

A measurement of Dijet Rates in Deep Inelastic Scattering at HERA

H1 Collaboration

Abstract

Dijet event rates, R_2, have been measured for deep inelastic ep scattering using data collected with the H1 detector in the years 1996-1997 corresponding to an integrated luminosity of 22 pb^{-1}. R_2 is shown as a function of x_B and Q^2 in the kinematic region $10^{-4} < x_B < 10^{-2}$ and $5 < Q^2 < 100\,\mathrm{GeV}^2$. The data are confronted with next-to-leading order QCD calculations using two different choices of the renormalization scale μ_r^2 and assuming a point-like structure of the virtual photon. While for $\mu_r^2 = Q^2$ the NLO predictions match the measured dijet rate within the rather large scale uncertainties, the choice $\mu_r^2 = Q^2 + E_t^2$ leads to a substantially lower but theoretically more reliable prediction demanding the inclusion of higher order processes. Therefore the data are compared to NLO QCD calculations which include a resolved structure of the virtual photon. In addition, the dependence of the measured dijet rates on the transverse energy requirement for the jets is studied in bins of x_B and Q^2 providing a highly differential measurement of R_2 for comparison to current fixed order and future resummed calculations.

Abstract: 997
Parallel session: 3
Plenary Talk: 11

Electronic Access: http://www-h1.desy.de/h1/www/publications/H1_sci_results.shtml

1 Introduction

The study of jets in deep-inelastic ep scattering (DIS) at HERA, colliding 27.5 GeV electrons on 820 GeV protons, provides a large phase space for testing perturbative QCD.

If QCD in next-to-leading order (NLO) is employed to confront theory with measurement, the dependence of the theoretical prediction on the choice of the renormalization scale μ_r^2 is expected to be small. However, the correct choice of μ_r^2 remains a matter of concern especially at low x_B and low Q^2 where higher orders in the perturbation series might be of more importance. For the study of dijet events in DIS at least two scales are suggested by the nature of the process, the first of which is the four-momentum transfer Q^2. The other possible scale for jet production is the transverse energy of the outgoing jets. The comparison of the H1 jet data with NLO predictions for these different scales is addressed by this paper. The H1 collaboration has measured the fraction R_2 of dijet events in all DIS events as a function of the Bjorken variable x_B in different regions of the four-momentum transfer Q^2.

2 The H1 Detector

A detailed description of the H1 apparatus is given elsewhere [1]. Those components essential for this analysis are briefly described in the following. The interaction area is surrounded by a tracking system of interleaved multi-wire proportional chambers and drift chambers which in total cover the polar angle[1] between $7^o < \theta < 155^o$. They provide the primary measurement of charged particles. A highly segmented liquid argon calorimeter, covering the polar angle $4^o < \theta < 154^o$, surrounds the tracking system, providing the measurement of both, electromagnetic and hadronic interacting particles. In the direction of large polar angles a lead scintillating-fiber calorimeter (SpaCal) [2] and a drift chamber (BDC), both covering the polar angle $153^o < \theta < 178^o$, enable a precise measurement of the scattered electron.

3 Data selection

The data used in the presented analysis were taken in the years 1996/97 with the H1 detector and correspond to an integrated luminosity of 22 pb^{-1}. DIS events relevant for this study are characterized by the electron being scattered into the SpaCal. An energy deposit of at least $6\,\mathrm{GeV}$ in the SpaCal and a loose track requirement is demanded in the trigger. The most energetic cluster in the SpaCal defines the electron candidate and events with a scattered electron of at least $9\,\mathrm{GeV}$ are accepted. The cluster position has to be between $156^o < \theta < 175^o$ such that it is well measured within the acceptance of the SpaCal and the BDC, which is used to measure the polar angle of the electron candidate. The event kinematics are then reconstructed from the energy and the polar angle of the scattered electron alone.

The hadronic final state is reconstructed from all remaining energy depositions in the SpaCal and the liquid argon calorimeter as well as from track momenta measured in the tracking system.

[1] Polar angles are defined with respect to the positive z-axis, the proton beam direction

While all clusters in the calorimeters are considered, the four momentum of a track is only allowed to contribute up to a momentum of $350\,\mathrm{MeV}$. The inclusion of tracks into the hadronic final state reconstruction substantially improves the energy measurement of the identified jets (see below).

Background to the DIS events arises from photoproduction, where the electron leaves the detector undetected and a particle from the hadronic final state is misidentified as the scattered electron, as well as from beam-gas and beam-wall interactions. Therefore additional cuts are applied to minimize the contamination by these background sources and the influence of QED radiation:

- The event must have a reconstructed vertex within $\pm 35\,\mathrm{cm}$ of its nominal position.
- The quantity $\sum(E - p_z)$ is calculated from the energy and the longitudinal momenta of scattered electron and the objects associated with the hadronic final state. The value of $\sum(E - p_z)$ is expected to be equal to twice the electron beam energy of 27.5 GeV. An undetected electron in a photoproduction event or initial state photon radiation will decrease the value of this observable. For this analysis $35 < \sum E - p_z < 70\,\mathrm{GeV}$ is required.

The phase space of the analysis is finally fixed by the following requirements:

- The four-momentum transfer Q^2 must be in the range $5 < Q^2 < 100\,\mathrm{GeV}^2$ and the Bjorken scaling variable x_B must be in the range $10^{-4} < x_B < 10^{-2}$.
- The inelasticity y must be greater than 0.1. The requirement of a minimum energy of the scattered electron of $9\,\mathrm{GeV}$ corresponds to an upper cut on y of 0.7 leading to a y-range of $0.1 < y < 0.7$.

In order to distinguish dijet events from the bulk of the DIS events, the objects of the hadronic final state described above are input to a jet algorithm. The jet search is performed in the photon-proton center of mass system using the inclusive k_t algorithm [3]. Dijet events are defined to have at least two jets fulfilling the following criteria: The transverse energy $E_{t,jet}$ of each jet has to be larger than $5\,\mathrm{GeV}$ and their pseudo-rapidity η as measured in the laboratory frame has to be between -1 and 2.5.

4 Correction of the data and systematic errors

The data are corrected for detector effects and effects of QED radiation using events simulated with the DJANGO/ARIADNE [4, 5] and RAPGAP [6] Monte-Carlo generators. Both give a satisfactory description of the event characteristics [7]. The mean of the predictions of these models was used for the bin-wise correction of the data. The difference between the correction factors obtained by the models and the mean is considered as a systematic error of the final result leading to an uncertainty well below 10%.

Additional systematic errors result from uncertainties of the hadronic energy scale of $\pm 4\%$ which leads to a typical error of 10% on the final result and constitutes the dominant error source. Other systematic uncertainties like that on the electromagnetic energy scale of the SpaCal or the measurement of the polar angle of the scattered electron are much smaller.

5 Comparison between data and theory

5.1 Comparison to NLO QCD calculations

The dijet rates are compared to NLO calculations using the DISENT [8] program which calculates the cross section for ep scattering to order $\mathcal{O}(\alpha_s^2)$ assuming the virtual photon to be point-like. To avoid infrared sensitivity of the predictions [9, 11], the transverse energies of the jets are required to be $E_{t,jet1} > 7\,\mathrm{GeV}$, $E_{t,jet2} > 5\,\mathrm{GeV}$. The corresponding dijet rates are shown in figure 1. The dijet rates increase for decreasing x_B as expected, since the available phase space increases with the invariant mass of the hadronic final state $W^2 \approx \frac{Q^2}{x_B}$.

In figure 1 the NLO QCD calculations are shown for two choices of the renormalization scale, namely $\mu_r^2 = Q^2$ and $\mu_r^2 = Q^2 + E_t^2$. The factorization scale is set to $\mu_f^2 = Q^2$ and the CTEQ4M [10] parton densities are used for the proton. The calculations have been corrected for hadronization effects which lower the prediction by approximately 10%.

The theoretical predictions describe the data for $\mu_r^2 = Q^2$ with scale uncertainties up to 30%, if μ_r^2 is varied by a factor of two. If $\mu_r^2 = Q^2 + E_t^2$ (where $E_t = (E_{t,jet1} + E_{t,jet2})/2$) is chosen, the NLO QCD calculations describe the data for large x_B and Q^2 only and clearly lie below the data for low x_B and low Q^2. In this case, however, the scale uncertainties are considerably smaller. The calculations leave room for introducing additional contributions to jet production, for example processes where the virtual photon becomes resolved and acts as a source of partons.

5.2 Contributions from a virtual photon structure?

In order to investigate a possible resolved contribution of the photon to dijet production, the data are compared to NLO QCD calculations using the program JETVIP [12]. For these studies the renormalization and factorization scale are set to $\mu_r^2 = \mu_f^2 = Q^2 + E_t^2$ and the SAS-1D[13] parton densities for the virtual photon are used. As shown in figure 2 the full calculation including all resolved and direct contributions leads to a better agreement with the data than a JETVIP calculation which only considers a point-like photon.

5.3 Dependence of R_2 on the transverse energy of the jets

To study the dependence of the dijet rate on the transverse energy of the jets, R_2 is measured as a function of the parameter Δ where the highest $E_{t,jet}$ satisfies $E_{t,jet1} > (5 + \Delta)$ GeV . Note that as $\Delta \to 0$ the cuts on the jets become symmetric and the NLO calculations become infrared sensitive. The measured R_2 as a function of Δ is presented in figure 3 for two bins in Q^2 and x_B.

At large x_B and large Q^2 and $\Delta \geq 1$ GeV, when staying away from the infrared sensitive region of the calculation, the NLO QCD calculations using DISENT describe the data well for both choices of μ_r^2 . In the low x_B,Q^2 regime the predictions only describe the data when choosing $\mu_r^2 = Q^2$. For $\mu_r^2 = Q^2 + E_t^2$ a reasonable agreement between the prediction and the measurement is only observed for $\Delta = 7$ GeV which is equivalent to the requirement of large transverse energies of the jets. Finally, the NLO calculations show a turnover for Δ below about 1 GeV whereas the data continue to increase towards $\Delta = 0$ showing the need for resummed calculations.

The two bins shown in figure 3 are part of a detailed scan of the phase space which is presented in figure 4. It is evident that for fixed Q^2 and decreasing x_B the NLO description fails to describe the data for $\mu_r^2 = Q^2 + E_t^2$ and that $\mu_r^2 = Q^2$ is favored by the data.

6 Summary

A measurement of the dijet rate R_2 in the phase space region $10^{-4} < x_B < 10^{-2}$ and $5 < Q^2 < 100\,\mathrm{GeV}^2$ has been presented. The dijet rate is described by NLO calculations if $\mu_r^2 = Q^2$ is chosen as the renormalization scale albeit at the cost of large scale uncertainties. If, however, $\mu_r^2 = Q^2 + E_t^2$ is chosen –which considerable reduces the scale uncertainties– a substantial contribution from other sources of dijet production is needed. When studying the contribution from resolved virtual photons it was found that its inclusion helps to describe the data.

The dijet rate has also been studied as a function of the transverse energy of the jets. As before when choosing $\mu_r^2 = Q^2 + E_t^2$ as renormalization scale the data at low Q^2 and x_B are only described for large transverse energies of the jets. For large values of Q^2 and x_B, however, the theory successfully matches the data and the choice of the scale variable is less important. The measurement is extended to a region of phase space where resummation is required in the calculations and provides an important reference for improved theoretical predictions.

References

[1] H1 collaboration *Nucl. Instrum. Methods* **386** (310) 1996.

[2] H1 SpaCal Group *Nucl. Instrum. Methods* **374** (149) 1996.

[3] S.D. Ellis and D.E Soper, *Phys. Rev.* **D 48** (3160) 1993.

[4] G.A. Schuler and H. Spiesberger, *Proceedings of the workshop on Physics at HERA*, eds. W. Buchmüller and G. Ingelmann, Hamburg (1992) 1419

[5] L. Lönnblad, *Comp. Phys. Comm.* **71** (15) 1992.

[6] H. Jung, *Comp. Phys. Comm.* **86** (147) 1995.

[7] R. Pöschl, *PhD thesis*, in preparation.

[8] S. Catani and M.H. Seymour *Nucl. Phys.* **B 485** (291) 1997.

[9] M. Klasen and G. Kramer *Phys. Lett.* **B 366** (385) 1996.

[10] H.L. Lai et al. , *Phys. Rev.* **D 55** (1280) 1997.

[11] S. Frixione and G. Ridolfi *Nucl. Phys.* **B 507** (315) 1997.

[12] B. Pötter, *Comp. Phys. Comm.* **119** (45) 1999.

[13] G.A. Schuler and T. Sjöstrand, *Z. Phys.* **C 68** (607) 1995

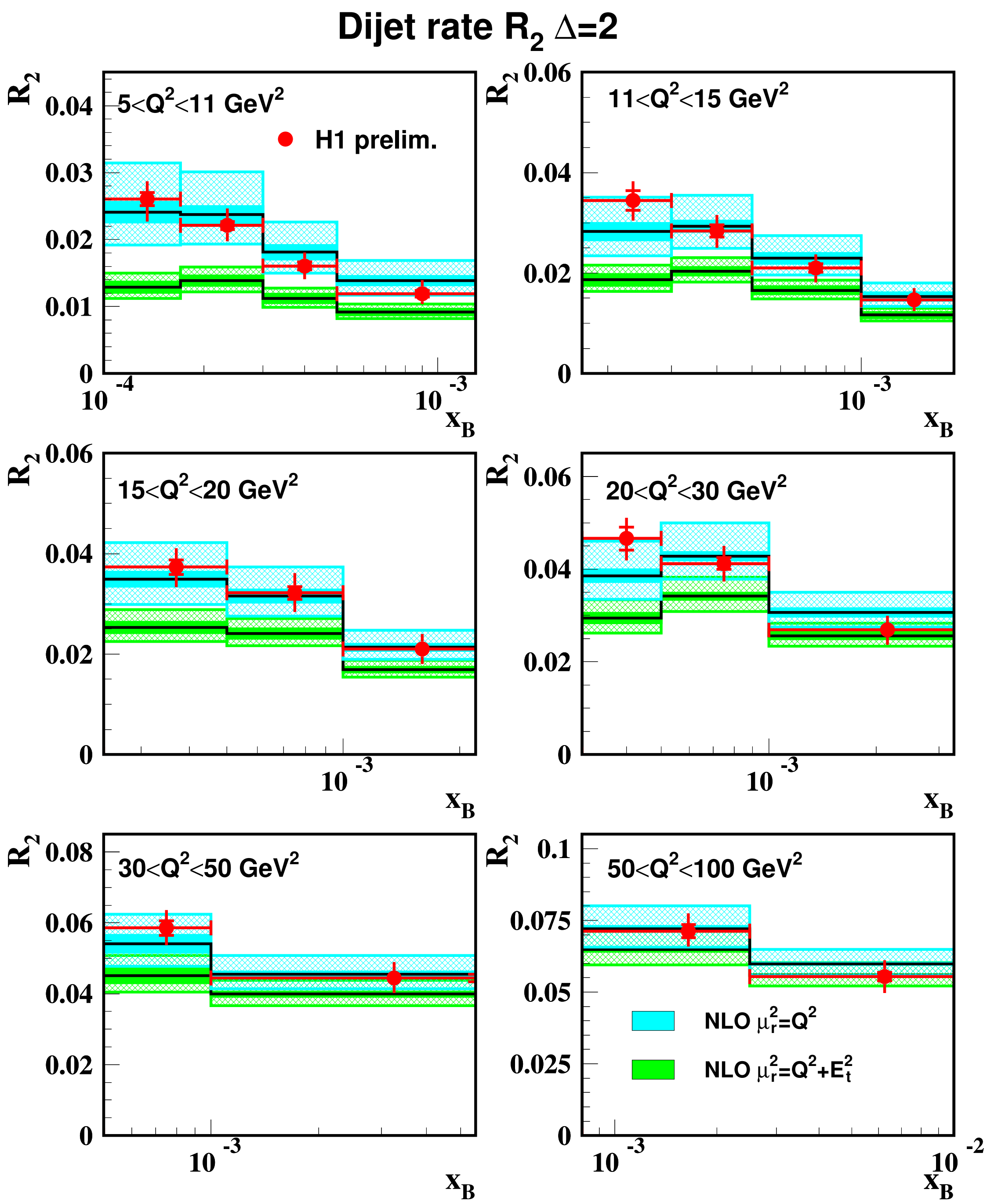

Figure 1: Dijet rate R_2 as a function of x_B in different bins of Q^2. The inner error bars of the data points indicate the statistical error only, the total error bars include also the statistical error added in quadrature. The data are compared to NLO QCD calculations which have been corrected for hadronization effects. The full bands indicate the uncertainty from the hadronization corrections and the hatched band indicate the error from the hadronization corrections and from the renormalization scale uncertainty added in quadrature.

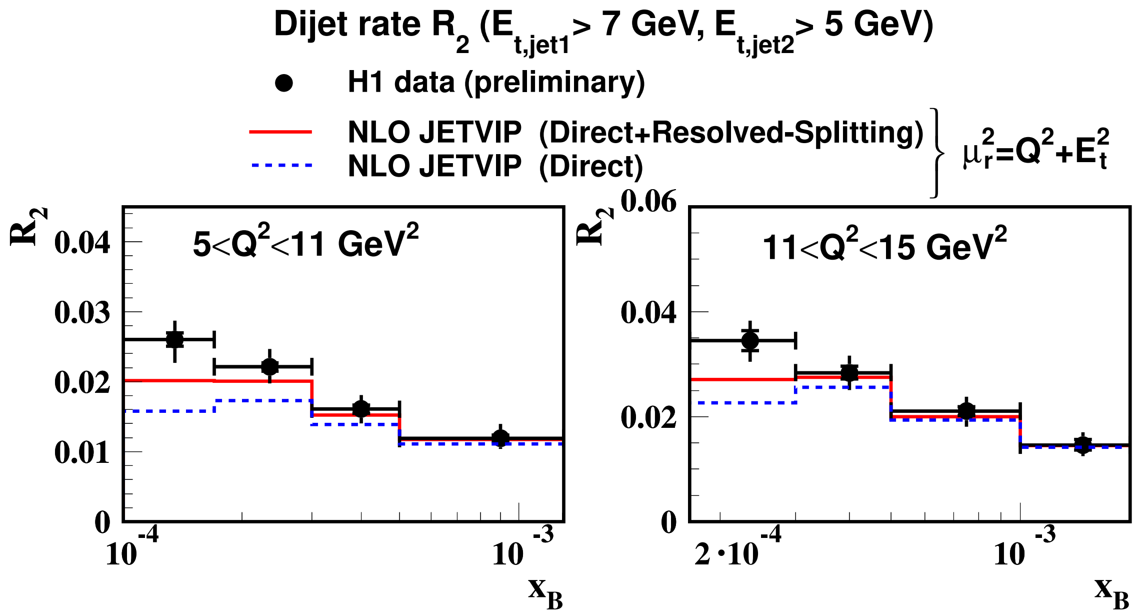

Figure 2: Dijet rate R_2 as a function of x_B in two different bins of Q^2. The data are compared to NLO QCD predictions assuming a direct coupling of the virtual photon and for predictions which include a virtual photon structure. The NLO QCD predictions have been corrected for hadronization effects.

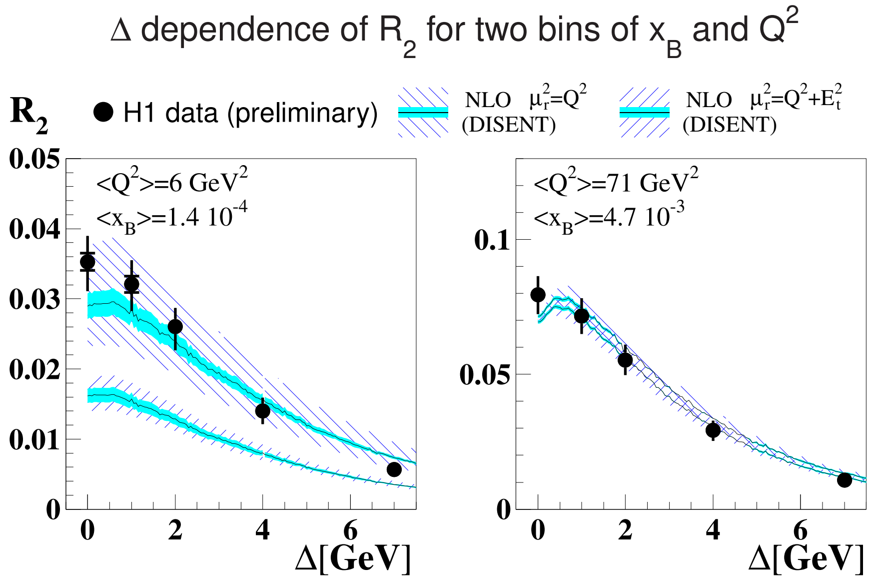

Figure 3: Dijet rate R_2 as a function of Δ in two extreme regions of Q^2 and x_B for this analysis. The variable Δ is defined by requiring $E_{t,jet} > (5+\Delta)$ GeV for the jet with the largest transverse energy. The data are compared to NLO predictions for two choices of the renormalization scale μ_r^2. The NLO predictions have been corrected for hadronization effects. The innermost band indicates the the error from the hadronization corrections and the full error band includes the scale uncertainty added in quadrature.

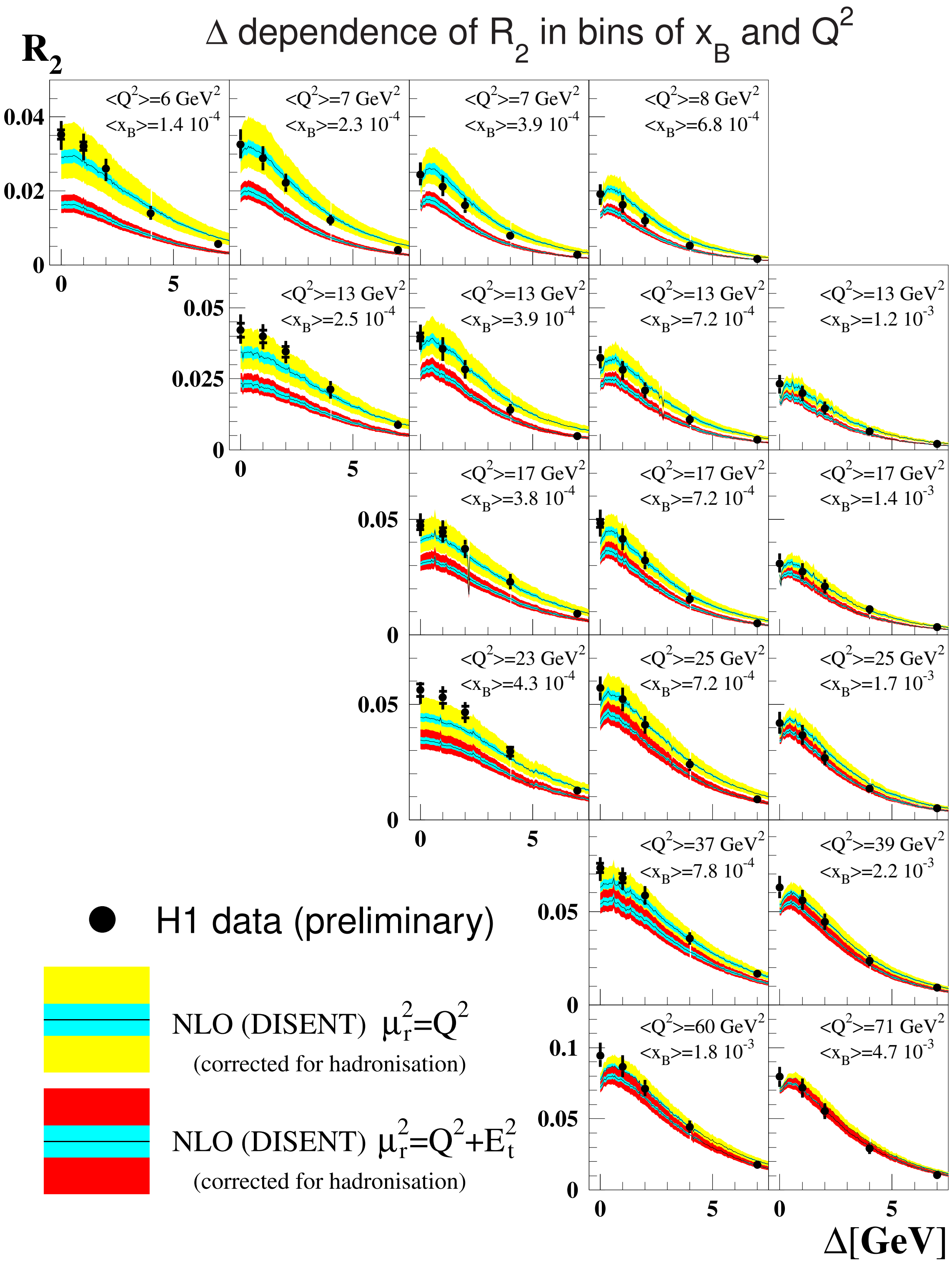

Figure 4: Dijet rate R_2 as a function of Δ in various regions of Q^2 and x_B. The two bins shown in figure 3 are included in this figure. The innermost band indicates the the error from the hadronization corrections and the full error band includes the scale uncertainty added in quadrature.